Full length article

Abrupt climatic events recorded by the Ili loess during the last glaciation in Central Asia: Evidence from grain-size and minerals

Yougui Song[a,d,*], Mengxiu Zeng[b], Xiuling Chen[c], Yue Li[a], Hong Chang[a], Zhisheng An[a], Xiaohua Guo[d]

[a] State Key Laboratory of Loess and Quaternary Geology, Institute of Earth Environment, Chinese Academy of Sciences, Xi'an 710061, China
[b] College of Geography and Environmental Sciences, Zhejiang Normal University, Jinhua 321004, China
[c] State Key Laboratory of Subtropical Mountain Ecology, College of Geographical Sciences, Fujian Normal University, Fuzhou 350007, China
[d] Geoluminescence Dating Research Laboratory, Department of Geosciences, Baylor University, Waco, TX 76798, USA

ABSTRACT

The loess record of Central Asia provides an important archive of regional climate and environmental changes. In contrast to the widely investigated loess deposits in the Chinese Loess Plateau, Central Asian loess–paleosol sequences remain poorly understood. Here, we present an aeolian loess section in the southern Ili Basin. Based on granularity and mineralogical analyses, we reconstruct climatic changes during the last glaciation. The results indicated that most of the abrupt climatic events (such as Dansgaard-Oeschger events and Heinrich events) were imprinted in this loess section, although their amplitudes and ages showed some differences. Compared with the millennial oscillations recoded in loess and stalagmites in East Asia, the arid Central Asia responded more sensitively to the warming events than to the cooling events. The shifting trajectory of westerlies across Central Asia played an important role in dust deposition during the stadials. The North Atlantic climatic signals may have been transmitted from Central Asia to the East Asian monsoon regions via the westerlies.

1. Introduction

Since the discovery of millennial-scale climate instability during the last interglaciation recorded in Greenland ice core (Bond et al., 1992; Bond and Lotti, 1995; Dansgaard, 1984; Dansgaard et al., 1993; Heinrich, 1988), there has been considerable effort to determine whether these climate events were a global phenomenon or just confined to the North Atlantic region, and also to identify the underlying mechanisms (Clement and Peterson, 2008; Heinrich, 1988; Rasmussen et al., 2014; Seierstad et al., 2014). Subsequently, similar abrupt climatic events have been reported from many diverse archives, such as loess sediments in the mid-latitude Chinese Loess Plateau (CLP) (Chen et al., 1997; Ding et al., 1999; Fang et al., 1999; Lu et al., 2004; Porter and An, 1995; Rao et al., 2013) or Southern Europe (Zeeden et al., 2017), lake sediments (Allen et al., 1999; Gorbarenko et al., 2007) and tropical marine sediments (Schulz et al., 1998) in low-latitude regions, or ice cores (Thompson et al., 1997) from the Tibetan Plateau.

The westerlies-dominated area of arid Central Asia is the furthest dust source from the oceans and plays an important role in global change (Fitzsimmons et al., 2017; Li et al., 2016a; Song et al., 2014; Sun, 2002; Zhao et al., 2013). Central Asia is also one of the most significant loess regions on Earth, located between the well-studied European loess sequences to the west and the extensive CLP region to the east (Machalett et al., 2008). This enables researchers to carry out interregional paleoclimatic investigations along a west-east transect across the entire Eurasian loess belt of the Northern Hemisphere. However, there are few reports of climatic change during the last glacial period in arid Central Asia. Widely distributed loess in the Tianshan mountains in Central Asia (Dodonov and Baiguzina, 1995; Li et al., 2015; Smalley et al., 2006; Song et al., 2014; Sun, 2002) has provided us with the opportunity to verify the last glacial climatic instability in Central Asia. The Ili basin is surrounded by the Tianshan mountains, and loess is widely distributed on the terraces and piedmonts (Song et al., 2014; Sun, 2002). Previous studies (Li et al., 2011, 2016a; Song et al., 2017; Ye et al., 2000; Zhao et al., 2013) in the Ili basin have also identified climatic events; however, due to geochronological limitations (E et al., 2012; Feng et al., 2011; Song et al., 2015, 2012; Yang et al., 2014) and a lack of reliable proxies (Li et al., 2017; Liu et al., 2012; Shi et al., 2007; Song, 2012; Song et al., 2010; Zhang et al., 2013) from the this region, the amplitude and frequency of climatic change and its possible driving mechanisms remain poorly understood. Here, based on an updated geochronology (Song et al., 2012), grain size and

* Corresponding author at: 97 Yanxiang Road, Xi'an 710061, Shaanxi, China.
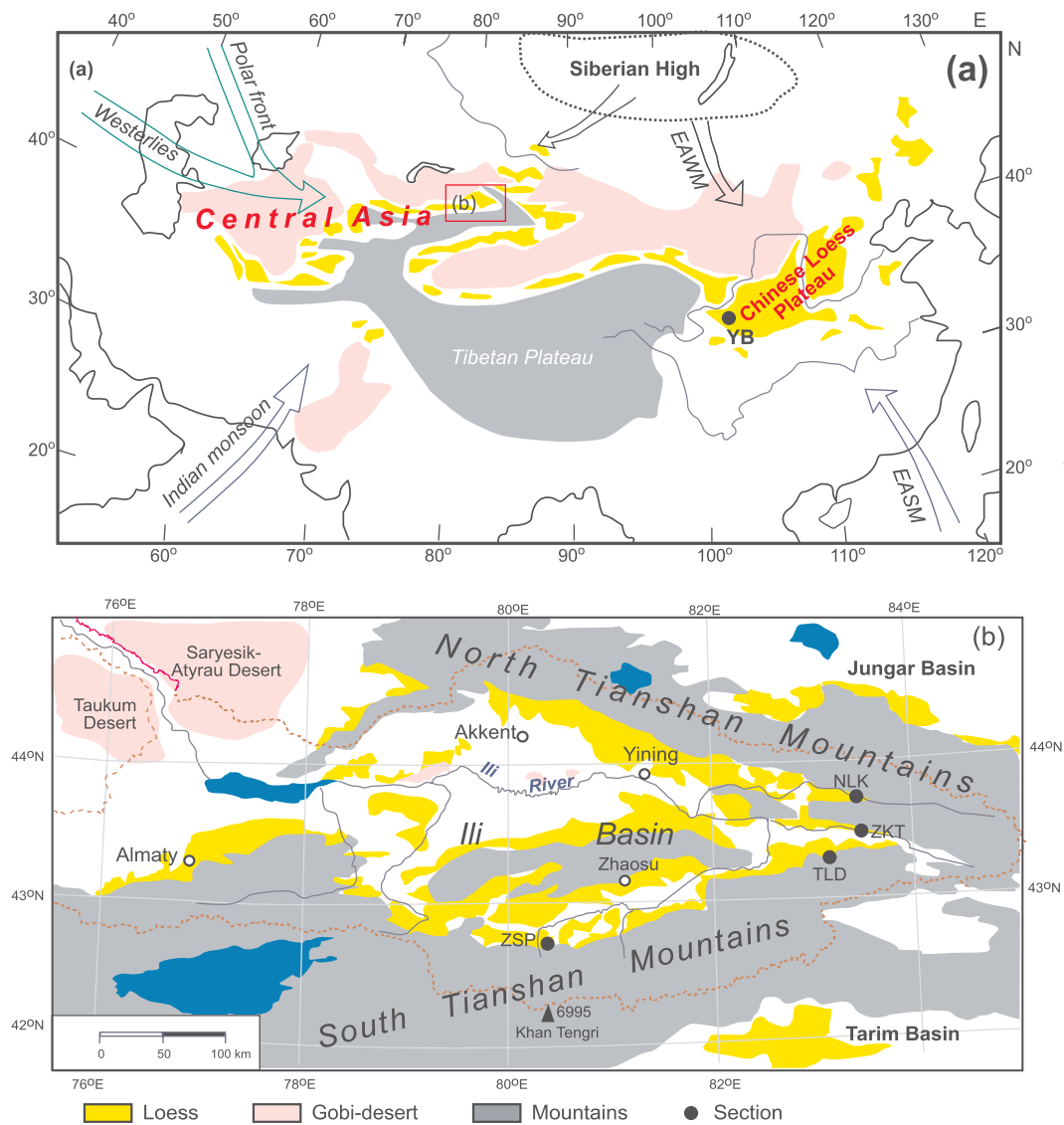 *E-mail addresses:* ygsong@loess.llqg.ac.cn, yougui_song@baylor.edu (Y. Song).

Fig. 1. Asian loess and Gobi desert distributions, and atmospheric circulation (a), and physical geography of the Ili basin (b). Modified from Song et al. (2010). Mentioned loess sections: YB: Yuanbao (Rao et al., 2013), NLK: Nileke (Song et al., 2015; Yang et al., 2014), ZKT: Zeketai (E et al., 2012; Feng et al., 2011), TLD: Talede (Kang et al., 2015; Liu et al., 2012).
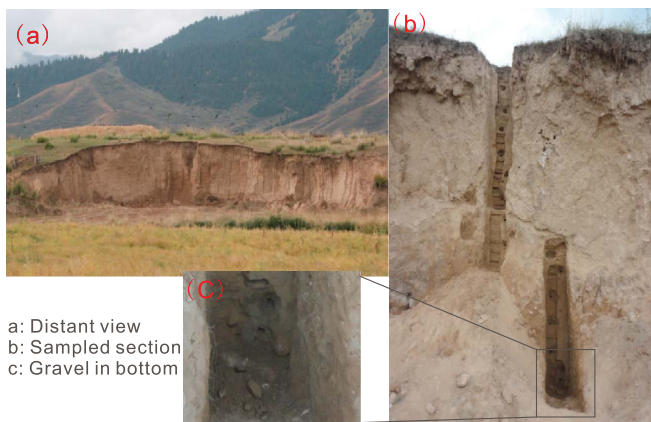

a: Distant view
b: Sampled section
c: Gravel in bottom

Fig. 2. Photographs of the Zhaosu Poma (ZSP) loess section.

mineralogy, we present a new loess section to determine the timing and characteristics of abrupt climatic events during the last glacial period.

2. Physical setting

The Ili basin is a Mesozoic-Cenozoic faulted depression, surrounded by the Tianshan orogenic belt which reaches altitudes > 3500 m. The topography of the Ili basin is shaped like a trumpet, with the mouth in the west; i.e., the altitudes are higher in the eastern part and lower in the western part, and the Kazakhstan Gobi Desert lies to the west (Fig. 1). The Ili River originates from north slope of Khan Tengri peak (6995 m a.s.l.), flows through the Ili Basin into the Kapchagay reservoir, before finally flowing to the west and into Balkhash Lake. Areas of Gobi desert are distributed around the Kapchagay Gorge and to the south of Akkent.

The Ili Basin is located in the inland region of the Eurasian continent and is thus far away from the ocean. The basin has a temperate semiarid continental climate and is primarily influenced by mid-latitude westerlies throughout the year (Li et al., 2011; Ye, 2001). The winter climate is mainly controlled by the intensity and position of the Asiatic polar front and Siberian high pressure cell (Fig. 1a), and is also influenced by the northern branch of the westerlies; the summer climate is
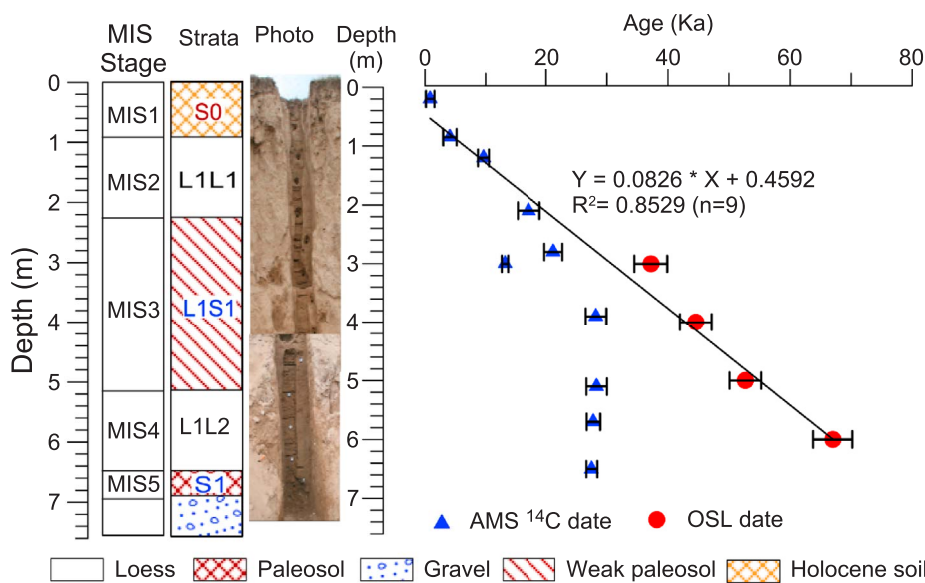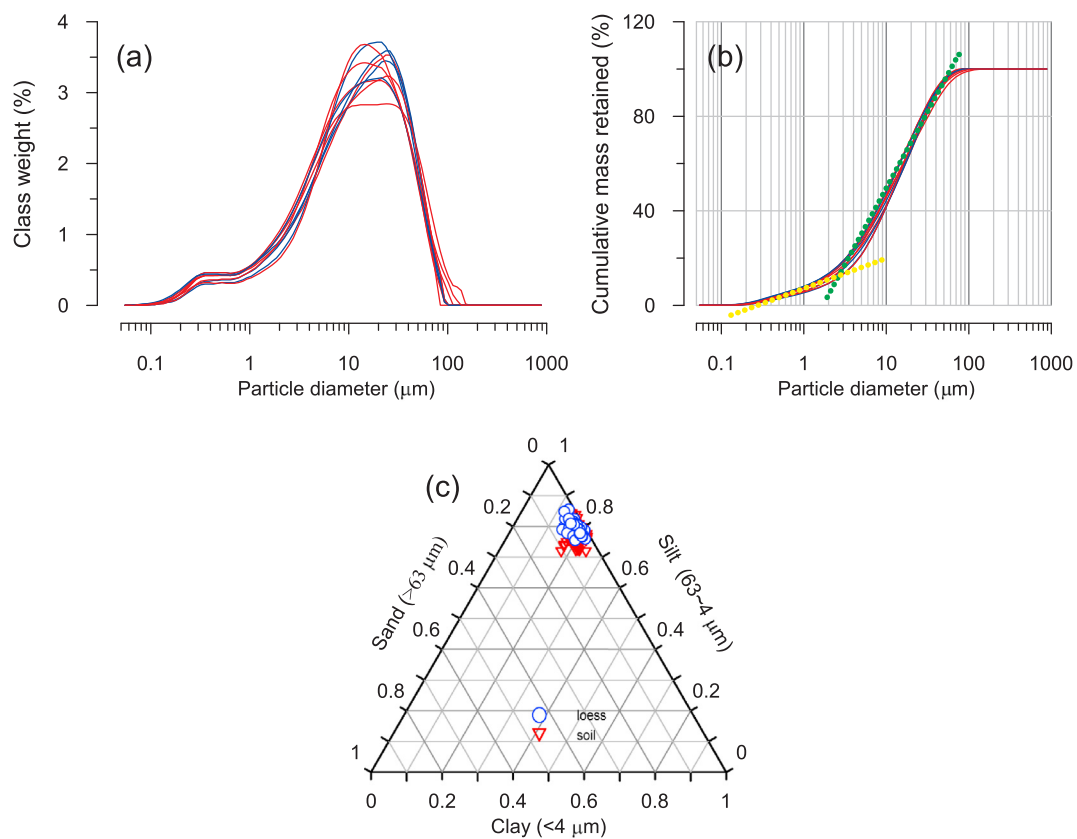
Y = 0.0826 * X + 0.4592
R² = 0.8529 (n=9)

Fig. 4. Grain-size distribution (a), cumulative curves (b) and ternary diagrams (c) of loess (blue) and (weak) soil (red) from the ZSP section, Ili Basin. (For interpretation of the references to colour in this figure legend, the reader is referred to the web version of this article.)

partially affected by the Indian low pressure cell, when the southern branch of the westerlies shifts northwards (Li, 1991). Cold, moist air mass influxes from the west to central Tianshan bring widespread precipitation (Aizen et al., 2001). Ice-core isotope records from Inilchek Glacier in the central Tianshan indicated that 87% of snow accumulation forms by precipitation originating from the Aral–Caspian closed basin, the eastern Mediterranean and Black Seas, and 13% from the North Atlantic (Aizen et al., 2006). Topography has a large influence on

the mean annual temperature (MAT) and mean annual precipitation (MAP) of the region. The MAT of the Ili Basin ranges from 2.6 to 10.4 °C, depending on the terrain. The Ili basin has the greatest MAPs in Xinjiang, because it is open on the west to humid airflow. The MAP ranges from 200 mm to 500 mm on the plains, but can reach 1000 mm in the mountain zones.

The soil in the Ili Basin is dominated by chestnut soil, chernozem and sierozem. Loess sediments are mainly distributed on hills,
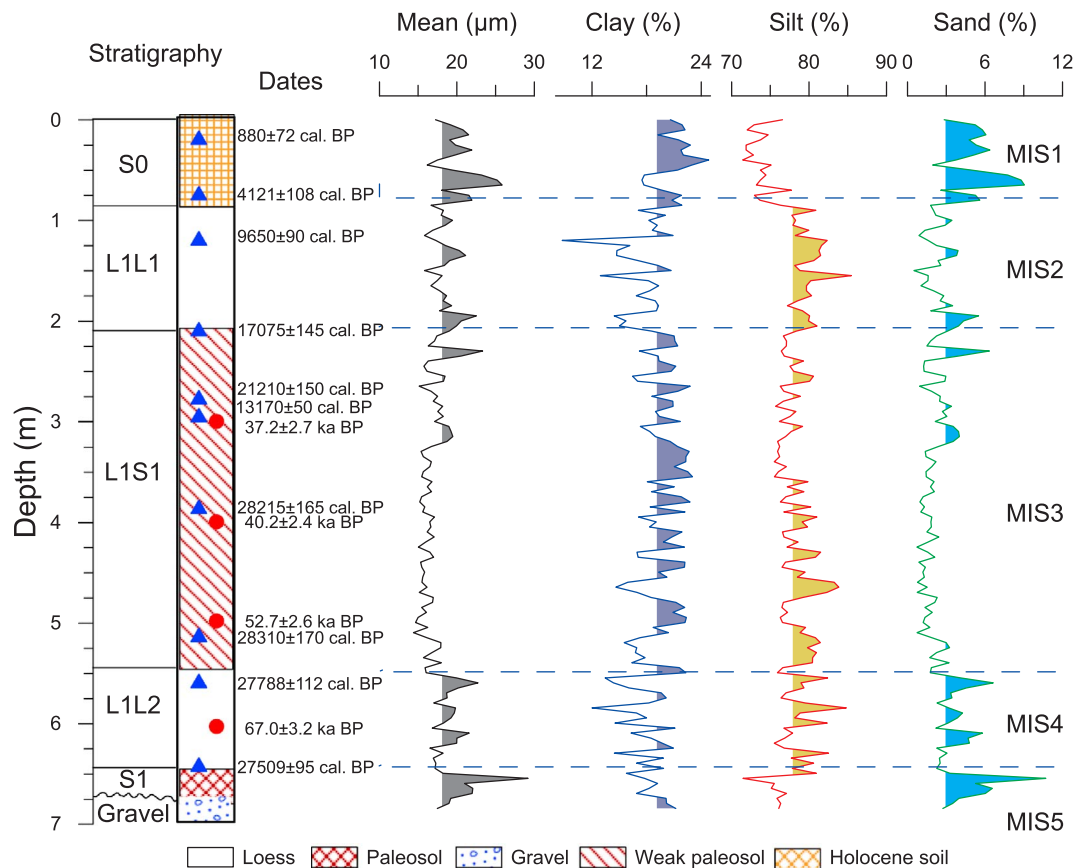
Fig. 5. Changes in grain-size parameters with depth of the ZSP section.

piedmonts and higher terraces, with thicknesses of meters to two hundred meters (Song et al., 2014). Because of the valley microclimate effect, the area possesses fairly distinct and complete vegetation types, comprising desert, montane-steppe, montane forest-meadow, subalpine meadow, alpine meadow and alpine cushion-like vegetation as elevation increases from the plain to the mountain, respectively (Hu, 2004).

3. Material and methods

3.1. Stratigraphy and dating

The Zhaosu (ZSP) loess section (42°41′40.4″ N, 80°15′16.3″ E, 1875 m a.s.l.) is situated on the second terrace of a tributary of the Tekes river (upper reaches of the Ili river), and lies in the steppe zone in the foothills of the Tianshan Mountains (Fig. 2). The 6.9 m-thick section can be divided into five pedostratigraphic units. Underlying the loess sequence are fluvial gravel sediments. Therefore, the paleosol in the lowermost section was affected by fluvial process. Detailed lithological descriptions and dating results were reported by Song et al. (2012). A total of 138 powdered samples were collected at 5 cm intervals through the section.

Previous geochronological work has revealed that this loess section has developed since the last glacial period (Song et al., 2012). The OSL ages are in agreement with the stratigraphy observed in the field (Fig. 3). Comparison between OSL and AMS ^{14}C dating of the Ili loess indicate that the OSL and radiocarbon ages agree well for ages younger than ca. 25 cal ka B.P. (^{14}C age), but beyond this age, the radiocarbon ages are underestimated and reversals because of by various carbon contaminations (Song et al., 2012), and 5 supplementary AMS ^{14}C dating samples confirm this underestimation (Fig. 3). New geochronological evidence also supports that OSL dating is applicable for constructing an accurate geochronology of late Quaternary loess in the Ili

basin (Kang et al., 2015; Song et al., 2015). Based on obtained OSL and AMS ^{14}C dates (< 25 ka cal B.P.), the grain size age model (Porter and An, 1995) was employed to establish the chronological sequence (Li and Song, 2011), yielding a basal age of 76 ka BP.

3.2. Grain-size analysis

The method of loess grain-size analysis followed Lu and An (1998a). Samples weighing 3–5 g were first treated with 30% hydrogen peroxide (H_2O_2) to remove organic matter, and then calcium carbonate was removed using 10% hydrochloric acid (HCl). The remainder was dispersed with 0.5 N sodium metaphosphate ($Na(PO_3)_6$) solution and oscillated in an ultrasonic bath for 10 min in order to completely separate the fine particles. The grain-size distributions were measured using a Malvern Mastersizer 2000 laser grain-size analyzer, which has a measurement range of 0.01–2000 μm with a 0.1Φ interval resolution. Replicate analyses indicate that the mean grain size has an analytical error of < 3%.

3.3. Mineralogy

To analyze the bulk mineral compositions, the air-dried loess sediments were ground by hand with an agate mortar and pestle to about 300 mesh size (< 40 μm), then the powder was scanned from 3 to 60° (2θ) with a Philips X'pert Pro (PW3071) X-ray diffractometer (XRD) using 40 mA, 40 kV generator settings and 1.540598 Å CuKa radiation. Minerals were identified with reference to patterns in the Powder Diffraction File (PDF2004) using Panalytical Highscore software, and the Levenberg-Marquardt (LM) method of qualitative analysis was applied to compute the contents of minerals mixed with corundum standard quantitative material (Zeng and Song, 2012, 2013a).
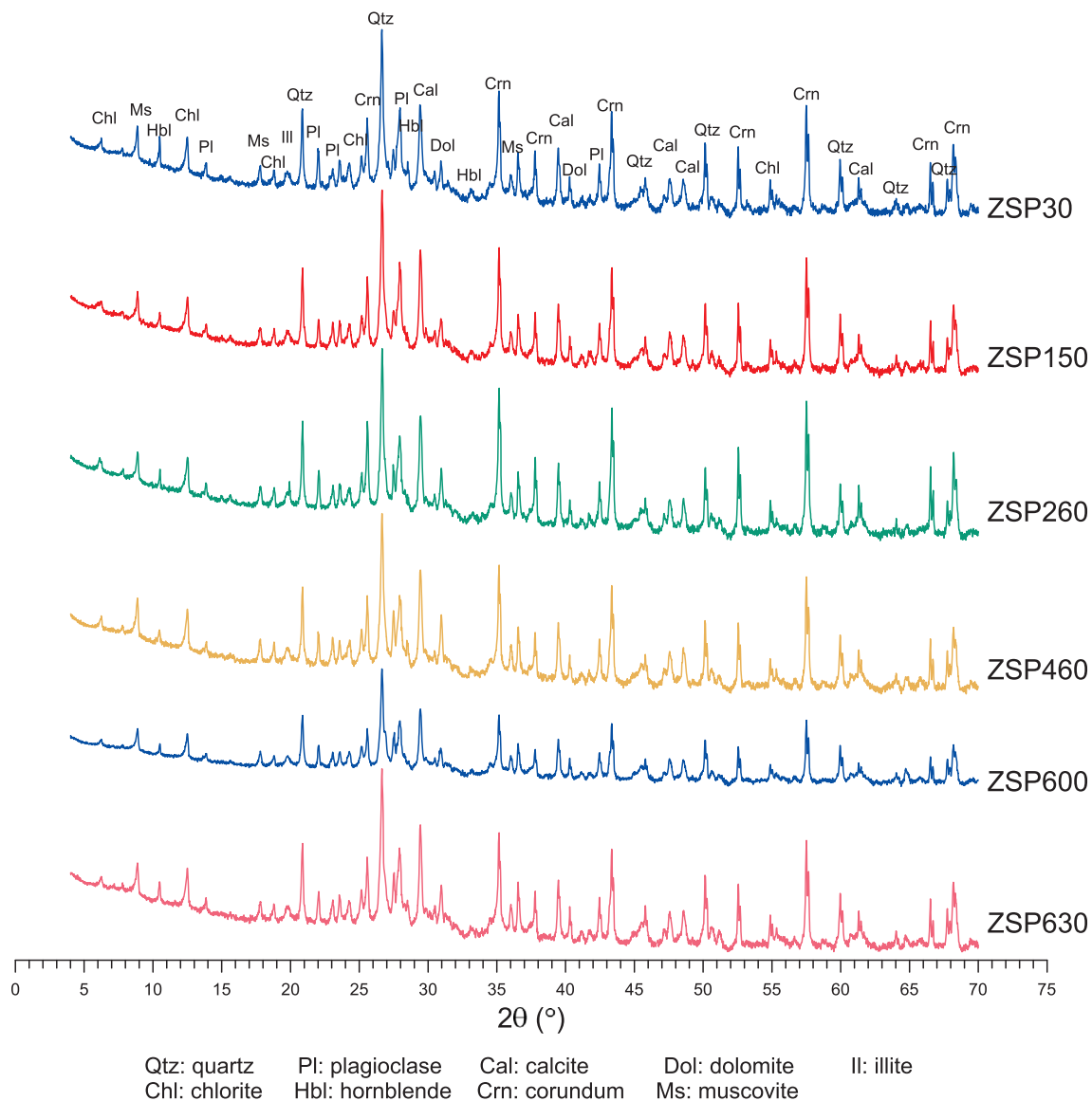
Fig. 6. Representative X-ray diffraction spectra of bulk loess samples in the ZSP section.

4. Results

4.1. Grain-size distribution

Grain-size analysis (Figs. 4 and 5) shows that ZSP loess is dominated by silt with an average content of 71.43%, ranging from 59.46% to 85.47%, representing the basic component of aeolian sediments. The clay fraction ranges from 12.02% to 24.80% (average 19.12%), while the sand fraction varies from 0.5% to 10.71% (average 2.87%). The grain-size distributions of the loess and (weak) paleosol samples in this section are generally consistent, and are characterized by unimodal distributions, positive skewness and long tails (Fig. 4a). The primary modes are fairly prominent and are concentrated between 10 and 50 μm, while the minor modes are at approximately 0.5 μm. Cumulative curves indicate two obvious sections with a boundary at around 2 μm (Fig. 4b). Grain size ternary diagrams indicate that the ZSP loess can be classified as silt, with several sandy-silt layers (Fig. 4c).

Variations in grain size of the ZSP loess section are characterized by 5 distinctive phases, which roughly correlate with the strata (Fig. 5). Generally, the weak paleosol L1LS1 developed during the last interstadial; this corresponds to marine isotope stage (MIS) 3 and is

characterized by the finest sediment with the smallest mean grain size, and its higher clay and lower sand contents. The Holocene soil (S0) and last interglacial S1 paleosol have relatively coarser fractions, perhaps due to the effects of fluvial processes. The grain sizes of loess units L1L1 (last deglaciation, MIS2) and L1L2 (MIS4) are moderate.

4.2. Mineral compositions

Representative XRD patterns of bulk loess samples are illustrated in Fig. 6. Over 10 species of minerals were identified in this loess section. The dominant mineral species are detrital minerals such as quartz, feldspar (plagioclase, K-feldspar, albite), hornblende and mica, while the minor minerals are carbonate minerals such calcite and dolomite. There are also small amounts of clay minerals such as chlorite and illite (Fig. 6). Mineral compositions of the loess and paleosols are given in Table 1 and Fig. 7. The average (N = 138) mineralogical composition in the studied section is 40.64% quartz, 14.97% calcite, 12.21% chlorite, 11.91% plagioclase, 3.64% K-feldspar, 2.54% dolomite, 3.8% hornblende, and 1.17% muscovite (Table 1). In general, the mineral composition of the ZSP loess is similar to that of the last glacial loess (L1) in the CLP (Jeong et al., 2008, 2011) although the average relative

Table 1

Mineral compositions of loess and paleosol samples from the ZSP section in the Ili basin and loess sections in the Chinese Loess Plateau.

Strata	Number	Content	Qtz	Pl	Kf	Ms	Chl	Cal	Dol	Hbl
S$_0$	19	Min/%	30.9	6.4	1.1	0.6	6.7	5.0	0.3	2.3
		Max/%	54.2	20.5	5.5	3.3	14.2	15.5	5.3	8.1
		Mean/%	38.9	10.5	2.6	1.0	9.9	9.5	1.5	5.5
		SD	6.0	3.8	1.2	0.6	2.1	3.4	1.3	1.9
L$_1$L$_1$	28	Min/%	30.1	7.9	1.0	0.7	5.5	8.9	0.5	1.9
		Max/%	57.2	20.9	8.3	4.2	15.6	24.8	4.6	6.5
		Mean/%	42.1	12.0	3.2	1.5	10.8	16.4	2.4	4.1
		SD	7.0	2.9	1.7	1.0	2.2	4.6	1.1	1.1
L$_1$S$_1$	58	Min/%	28.5	5.1	1.0	0.4	8.3	9.5	0.3	1.0
		Max/%	57.8	24.9	9.6	5.2	18.8	28.2	6.2	6.5
		Mean/%	40.2	11.5	4.1	2.0	13.2	15.3	3.0	3.3
		SD	7.1	3.8	2.1	1.1	2.2	3.8	1.2	1.2
L$_1$L$_2$	26	Min/%	33.4	7.3	1.4	0.8	8.9	7.9	0.3	1.5
		Max/%	51.1	19.4	10.1	6.6	19.6	25.3	5.1	5.3
		Mean/%	42.1	12.8	3.8	1.9	12.9	16.8	2.5	3.0
		SD	5.2	3.6	1.9	1.5	2.7	3.9	1.1	1.1
S$_1$	7	Min/%	29.3	9.3	2.8	0.9	11.7	8.5	1.3	3.6
		Max/%	46.0	23.2	5.1	3.8	15.1	19.2	3.9	7.0
		Mean/%	38.4	15.4	3.8	1.9	13.5	15.0	2.5	5.3
		SD	7.0	5.8	0.9	1.1	1.4	4.3	0.9	1.5
Total	138	Min/%	28.5	5.1	1.0	0.4	5.5	5.0	0.3	1.0
		Max/%	57.8	24.9	10.1	6.6	19.6	28.2	6.2	8.1
		Mean/%	40.6	11.9	3.6	1.7	12.2	15.0	2.5	3.8
		SD	6.6	3.8	1.9	1.2	2.6	4.5	1.2	1.5
JZT[*]		Mean/%	41.4	12.1	3.7	1.8	12.3	16.1	2.6	3.5
ZSP L1	112	Mean/%	32.7	14.3	5.0		3.8	11.9	2.0	2.0
CLP L1	24	Mean/%	34.9	15.3	5.0		4.3	11.6	3.3	1.9
JZT[*] L1	13	Mean/%	33.1	14.9	4.7		4.1	14.1	2.1	1.9
DDL[**] L1	7	Mean/%	31.1	14.3	4.9		4.6	13.6	1.8	2.1
BS[**] L1	2	Mean/%	31.7	12.9	5.3		2.4	8.2	0.7	2.1

Qtz: quartz; Cal: calcite; Chl: chlorite; Pl: plagioclase; Hbl: hornblende; Kf, K-feldspar; Dol: dolomite; Ms: muscovite.

  * Data source: JZT: from Jeong et al. (2008).

  ** Data source: LJP, DDL, BS: from Jeong et al. (2011).

contents are different to some extent (Table 1). The obvious difference in the ZSP loess is that the abundances of quartz, chlorite, calcite and hornblende are greater than those of the L1 loess of the CLP (Table 1), indicating a weak weathering process. The variations in dolomite and quartz contents are characterized by large amplitudes and high frequency (Fig. 7).

5. Discussion

5.1. Interpretation of grain size

Grain-size of Chinese loess has been widely used as a proxy of past variations in both aeolian dynamics and patterns of atmospheric circulation (An et al., 1991; Sun et al., 2012), and the coarse/fine fractions are regarded as an index of winter/summer monsoon intensity (Lu and An, 1998b). Sun et al. (2004) further suggests that the coarse component provides an indicator of the source area aridity and the frequency of dust storms related to low-altitude northwesterly winds. The fine component probably represents the background dust load of the atmosphere and provides an estimate of the upper air westerly air stream intensity. On millennial timescales, evidence for rapid grain-size variations in the loess has been interpreted as a possible consequence of Heinrich ice-raft events and the Dansgaard/Oeschger (D-O) events (Porter and An, 1995; Rousseau et al., 2007; Sun et al., 2012). Arid Central Asia is an important dust source region in Asia and even the Northern Hemisphere. Because of the trumpet-shaped topography of the Ili basin, the coarse component is generally interpreted to have originated from proximal sources including fluvial sediments in the Ili

drainage and to have been blown and transported by dust storms via strong, local low-altitude atmospheric circulation (Li et al., 2017, 2016b; Shi and Dong, 2007). Size-differentiated REE characteristics from the Ili Basin indicates that coarse fractions are effective tracers for tracking changes in proximal dust sources and regional boundary level circulations, and the fine particles are sensitive indicators for distinguishing dust particles transported over long distances (Chen et al., 2017). The cold and dry climate are unfavorable to pedogenesis and therefore to the production of fine components; therefore, the fine component ($< 10\,\mu m$) of loess is regarded as an indicator of the strength of the Westerlies (Li et al., 2016a; Shi and Dong, 2007; Ye et al., 2000). The stronger the wind, the faster the dust is deposited, such that the fine fraction of the loess will decrease, and the coarse component will increase.

However, compared with grain size patterns of loess-paleosol sequences from the CLP, we observed that sand contents are high in paleosol layer (S1 and S0) and low in loess layers (Fig. 5). River erosion power maybe a reasonable explanation for the higher sand contents, which is similar to that of the relationship between Yellow River formation and dust deposition in the CLP (Nie et al., 2015). During interglacial period, climate was wetter, and river could erode more materials and the products of erosion could be blown to the terraces and piedmonts especially during strong dust storm periods. When climate was dry in glacial periods, river had less power to erode bedrocks, so less sand was available to be transported to the deposition region, and the proximal coarser components percentage decreased.

5.2. Palaeoenvironmental significance of minerals

Carbonates in loess sediments consist mostly of calcite and dolomite. Calcite is generally formed during pedogenesis by leaching, accumulation and crystallization, while dolomite is primarily a detrital material that reflects dust source regions (Liu, 1985; Yang et al., 2000). Calcite is diffluent in soil and thus becomes a common authigenic component. Pedologic studies indicate that the depth of the calcic horizon in modern soils of arid to semiarid areas has a strong, positive relationship with precipitation (Chen et al., 2007), in other words, leaching depth in loess is largely due to the local precipitation characteristics and is consequently regarded as a sensitive index of summer monsoon climate. However, grain size and micromorphological analysis have shown that there still exist many detrital calcites in the coarse fractions, reflecting source region conditions (Fang et al., 1994; Wen, 1989; Zeng and Song, 2013b). It is hard to quantitatively distinguish the contributions of authigenic or detrital calcite. This may bias the reconstruction of climatic change from total carbonate contents measured with the gasometric method or calcite contents (Chen et al., 2007). Dolomite does not readily dissolve in soil water and thus is mostly detrital in origin (Yang et al., 2000). The d value ($< 2.9\,Å$) of dolomite [1 1 0] also implies a detrital source (Chen and Li, 2011). Quartz, with its stable physical and chemical properties, is one of the most resistant components of loess deposits, and remains largely unaffected during the post-deposition and weathering processes. Quartz in aeolian loess sediments is derived from primary dust, thereby reflecting the dust source and transport dynamics. Thus, quartz content can be considered as a proxy for paleowind strength. Quartz on the CLP has been employed as a reliable proxy indicator of winter monsoon strength (Porter and An, 1995; Sun et al., 2006; Xiao et al., 1995). In other words, the changes in aeolian loess composition are mainly related to the dust source and wind strength. Previous heavy mineral and geochemical analyses have indicated that the dust provenance has not changed since the last glacial period (Song et al., 2014; Ye, 2001; Zhang et al., 2013). Therefore, the variation of dolomite/quartz mostly reflects the intensity of dust transportation by the westerlies. Specifically, stronger westerlies will cause more dust deposition and will transport more dolomite. The similarity between trends in quartz and dolomite (Fig. 7) also confirms this reasonable interpretation.
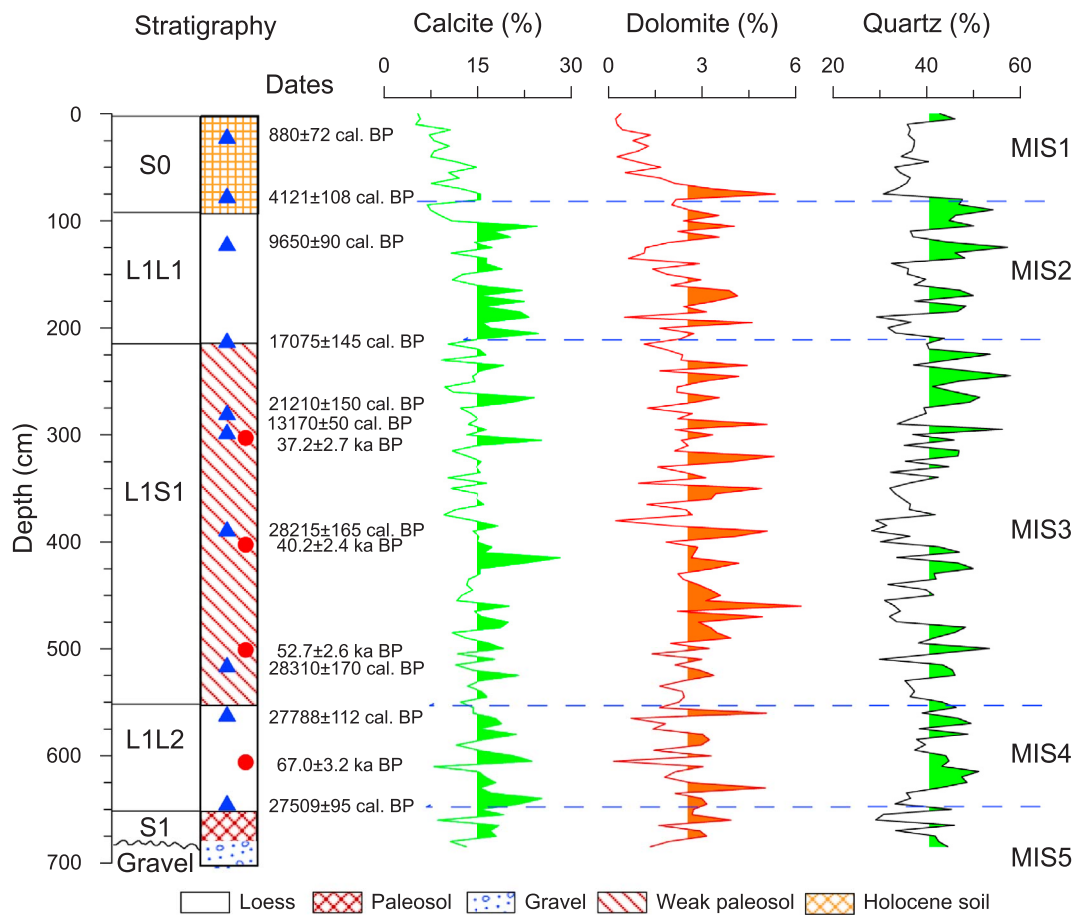
Fig. 7. Variations of minerals with depth in the ZSP section.

5.3. Climatic changes during the last glacial period

Because the Holocene soil (MIS1) may be affected by modern weathering process and the bottom S1 paleosol (MIS5) was mingled with fluvial sediments. We focus on discussing the climatic change in the last glacial period from MIS4 to MIS2. Both the particle size (Fig. 5) and mineral records (Fig. 7) during this interval show large-amplitude and high-frequency fluctuations. During MIS4, high coarse fractions (> 40 µm) and dolomite/quartz show strengthening westerlies in cold-dry condition, which lead to the transport of much coarser dust and development of stronger dust storms. Previous studies indicated reciprocal glacial-interglacial influences of the zonal westerlies and the Asiatic high on the aeolian dust transport in central Asia (Machalett et al., 2008). The Ili Basin is located at the core of the belt of westerlies (Fig. 1), where a strengthening polar front and Siberian High will force the westerlies southwards, and the strengthening local surface wind will intensify dust storms in cold condition. During MIS3, coarse fractions decreased dramatically (especially during MIS3b and MIS3c) and the mean grain sizes stayed at their smallest values (Fig. 5), indicating that the climate in the Ili basin is mainly controlled by westerlies under a relatively stable atmospheric circulation. Polar front and Siberian High retreat northward. The changes of various minerals have no obvious trend, although there are high-frequency oscillations. The content of fine fractions, quartz and dolomite contents began to decrease during MIS2, corresponding to slightly decreasing temperature or increasing ice volume (Fig. 8). A recurrent southward advance of polar front and Siberian High invaded the Ili basin during the cooling stadial. In general, the climatic changes in glacial-interglacial orbital timescale are synchronous with global glacial-interglacial change on orbital time scales. The shifting location of westerlies in Central Asia played an

important role in dust deposition during the stadials.

5.4. Abrupt climatic events and their correlation with regional and global records

As early as 1980s, Greenland ice core revealed that the last glacial period was characterized by abrupt climate changes that recurred on millennial time scales (Bond et al., 1992; Bond and Lotti, 1995; Dansgaard, 1984; Dansgaard et al., 1993; Heinrich, 1988). There are twenty-five of these distinct cooling-warming oscillations (D-O cycles) (Dansgaard, 1984; Dansgaard et al., 1993). Related to some of the coldest intervals between D-O cycles were six distinctive Heinrich (H) events recorded in North Atlantic marine sediments as ice-rafted debris layers with a large amount of coarse-grained sediments derived from land (Heinrich, 1988). When comparing these proxies with North Greenland ice core records, we find that our results can be well correlated with those of oxygen isotopes (NGRIP_members, 2004) and temperature (Rasmussen et al., 2014) (Fig. 8a). Frequent fluctuations of fine fraction and minerals during the last glaciation can be correlated with the climatic events (D-O and H events). The abrupt events generally correspond to peaks in quartz and dolomite contents and in fine size fraction (Fig. 8b–d). Most of Heinrich events can be correlated with lower finer fractions and quartz contents, albeit with some age differences which may be caused by sample resolution and dating errors. In term of amplitudes and frequency of changes, mineral compositions are relatively more sensitive to climatic changes. The above evidence provides firm support for the preservation of North Atlantic millennial scale abrupt climate events in the Ili loess. However, we note that not all troughs, for example, those around 16 ka and 65 ka in fine fraction curve, correlate with Heinrich events in the North Atlantic, implying
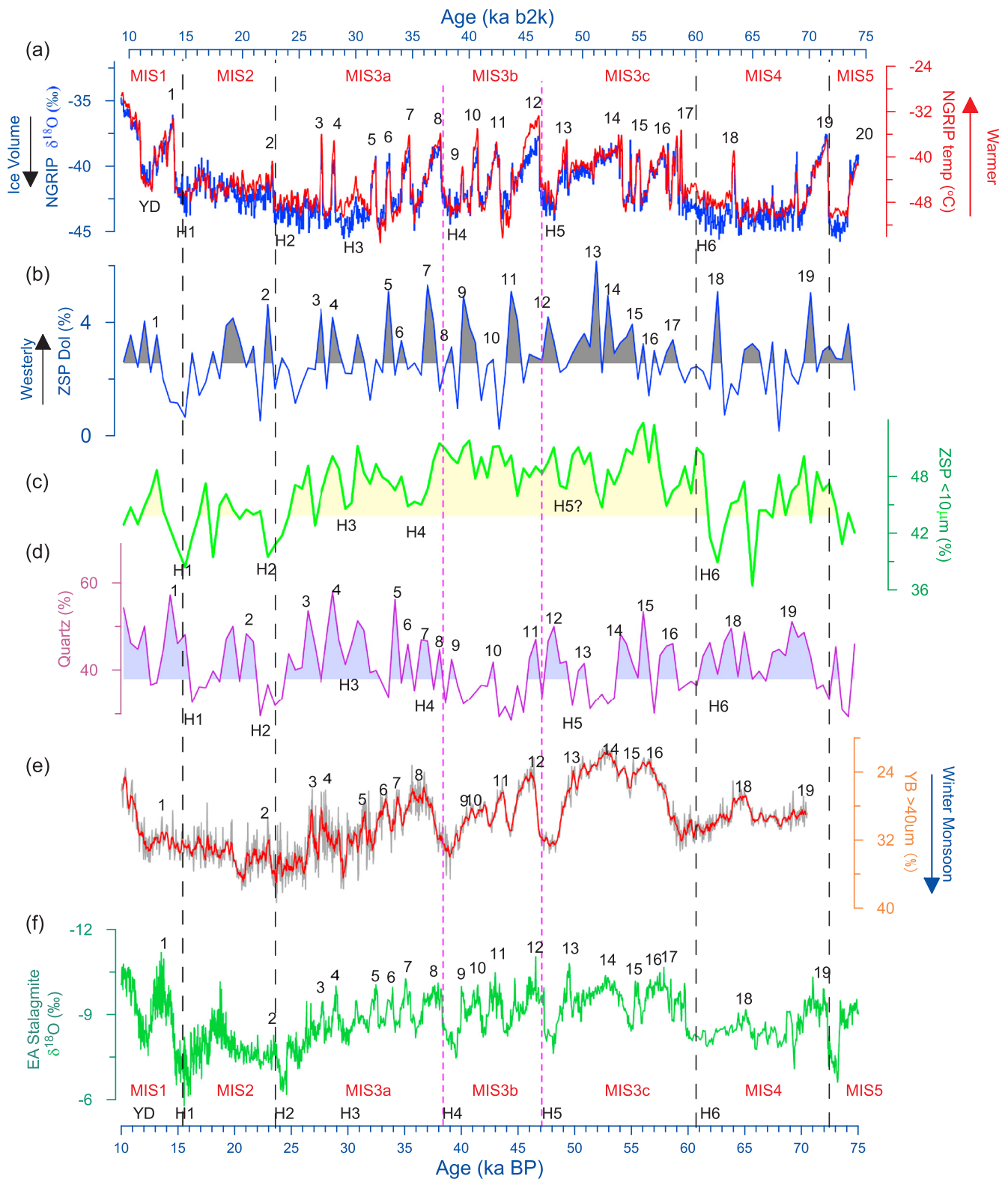
Fig. 8. Comparison of grain size and minerals records from the ZSP loess with Greenland ice core and other records. (a) δ¹⁸O (blue line) (NGRIP_members, 2004) and reconstructed temperature (red line) (Rasmussen et al., 2014) from the NGRIP ice core; (b) Dolomite contents (blue), (c) grain size (< 10 μm), (d) quartz content; (e) Yuanbao loess in the western CLP (Rao et al., 2013), (f) stalagmites in East China (Cheng et al., 2016). Black Arabic numerals indicate the interstadial events. (For interpretation of the references to colour in this figure legend, the reader is referred to the web version of this article.)

differences in regional conditions such as atmospheric circulation and topography. Millennial scale climate oscillations were also recorded in the Lower Danube loess in East Europe (Zeeden et al., 2017) and in the

loess from the Chinese Loess Plateau in East Asia (Fang et al., 1999; Lu et al., 2004; Porter and An, 1995).

In order to identify how the westerlies transmit North Atlantic

climatic signals to East Asia through Central Asia, we compared these records with loess (Rao et al., 2013) and stalagmites (Cheng et al., 2016) archives from East Asia (Fig. 8). Mineral records (dolomite and quartz) in Central Asia seem more sensitive to interstadial warm events (Fig. 8b, d), which are much clearer than those observed in loess and stalagmite records from East Asia. Meanwhile, the particle size in loess deposits from the CLP (Fig. 8e) is able to distinguish the abrupt events, and the stalagmite record (Fig. 8f) seems more susceptible to cold events. The range of climate variations indicated by loess and stalagmite records from East Asia was smaller than that recorded in Greenland. The low amplitude of climatic variations in East Asia was probably caused by the small range of temperature change relative to that in Greenland and weakening monsoon response to temperature changes (Chen et al., 1997). Therefore, North Atlantic climatic signals may be transmitted from Central Asia to East Asian monsoon regions via the westerlies.

6. Conclusions

Based on granularity and mineral analyses, we reconstructed climatic change during the last glaciation. The results indicated that most of the abrupt climatic events (such as Dansgaard-Oeschger events and Heinrich events) were imprinted in the loess records, although their amplitudes and ages showed some differences. The shifting location of westerlies in Central Asia played an important role in dust deposition during the stadials. Furthermore, the abrupt events in the Ili loess were much clearer than those preserved in loess and stalagmite records in East Asia. The North Atlantic climatic signals may have transmitted from Central Asia to East Asian monsoon regions via the westerlies.

References

Aizen, E.M., Aizen, V.B., Melack, J.M., Nakamura, T., Ohta, T., 2001. Precipitation and atmospheric circulation patterns at mid-latitudes of Asia. Int. J. Climatol. 21, 535–556.

Aizen, V.B., Aizen, E.M., Joswiak, D.R., Fujita, K., Takeuchi, N., Nikitin, S.A., 2006. Climatic and atmospheric circulation pattern variability from ice-core isotope/geochemistry records (Altai, Tien Shan and Tibet). Ann. Glaciol. 43, 49–60.

Allen, J.R.M., Brandt, U., Brauer, A., Hubberten, H.-W., Huntley, B., Keller, J., Kraml, M., Mackensen, A., Mingram, J., Negendank, J.F.W., Nowaczyk, N.R., Oberhänsli, H., Watts, W.A., Wulf, S., Zolitschka, B., 1999. Rapid environmental changes in southern Europe during the last glacial period. Nature 400, 740–743.

An, Z.S., Kukla, G.J., Porter, S.C., Xiao, J.L., 1991. Magnetic susceptibility evidence of monsoon variation on the Loess Plateau of central China during the last 130,000 years. Quat. Res. 36, 29–36.

Bond, G.C., Lotti, R., 1995. Iceberg discharges into the north Atlantic on millennial time scales during the last glaciation. Science 267, 1005–1010.

Bond, G., Heinrich, H., Broecker, W., Labeyrie, L., McManus, J., Andrews, J., Huon, S., Jantschik, R., Clasen, S., Simet, C., Tedesco, K., Klas, M., Bonani, G., Ivy, S., 1992. Evidence for massive discharges of icebergs into the North Atlantic ocean during the last glacial period. Nature 360, 245–249.

Chen, J., Li, G., 2011. Geochemical studies on the source region of Asian dust. Sci. China Earth. Sci. 54, 1279.

Chen, F.H., Bloemendal, J., Wang, J.M., Li, J.J., Oldfield, F., 1997. High-resolution multi-proxy climate records from Chinese loess: evidence for rapid climatic changes over the last 75 kyr. Palaeogeog. Palaeoclimatol. Palaeoecol. 130, 323–335.

Chen, X., Fang, X., An, Z., Han, W., Wang, X., Bai, F., Hong, Y., 2007. An 8.1Ma calcite record of Asian summer monsoon evolution on the Chinese central Loess Plateau. Sci. China Ser. D – Earth Sci. 50, 392–403.

Chen, X., Song, Y., Li, J., Fang, H., Li, Z., Liu, X., Li, Y., Orozbaev, R., 2017. Size-differentiated REE characteristics and environmental significance of aeolian sediments in the Ili Basin of Xinjiang, NW China. J. Asian Earth Sci. 143, 30–38.

Cheng, H., Edwards, R.L., Sinha, A., Spotl, C., Yi, L., Chen, S., Kelly, M., Kathayat, G.,

Wang, X., Li, X., Kong, X., Wang, Y., Ning, Y., Zhang, H., 2016. The Asian monsoon over the past 640,000 years and ice age terminations. Nature 534, 640–646.

E, C.Y., Lai, Z.P., Sun, Y.J., Hou, G.L., Yu, L.P., Wu, C.Y., 2012. A luminescence dating study of loess deposits from the Yili River basin in western China. Quat. Geochronol. 10, 50–55.

Clement, A.C., Peterson, L.C., 2008. Mechanisms of abrupt climate change of the last glacial period. Rev. Geophys. 46, RG4002, doi:4010.1029/2006RG000204.

Dansgaard, W., 1984. North Atlantic climate oscillations revealed by deep Greenland ice cores. In: Takahashi, J.E.H.T. (Ed.), Climate Processes and Climate Sensitivity. American Geophysical Union, Washington, DC, pp. 288–298.

Dansgaard, W., Johnsen, S.J., Clausen, H.B., Dahl-Jensen, D., Gundestrup, N.S., Hammer, C.U., Hvidberg, C.S., Steffensen, J.P., Sveinbjornsdottir, A.E., Jouzel, J., Bond, G., 1993. Evidence for general instability of past climate from a 250-kyr ice-core record. Nature 364, 218–220.

Ding, Z.L., Ren, J.Z., Yang, S.L., Liu, T.S., 1999. Climate instability during the penultimate glaciation: evidence from two high-resolution loess records, China. J. Geophys. Res. Solid Earth 104, 20123–20132.

Dodonov, A.E., Baiguzina, L.L., 1995. Loess stratigraphy of central Asia: paleoclimatic and palaeoenvironmental aspects. Quat. Sci. Rev. 95, 707–720.

Fang, X., Li, J., Derbyshire, E., Fitzpatrick, E.A., Kemp, R.A., 1994. Micromorphology of the Beiyuan loess-paleosol sequence in Gansu Province, China: geomorphological and paleoenvironmental significance. Palaeogeog. Palaeoclimatol. Palaeoecol. 111, 289–303.

Fang, X.M., Ono, Y., Fukuksawa, H., Pan, B.T., Li, J.L., Guan, D.H., Oi, K.C., Tsukamoto, S., Torii, M., Mishima, T., 1999. Asian summer monsoon instability during the past 60,000 years: magnetic susceptibility and pedogenic evidence from the western Chinese Loess Plateau. Earth Planet. Sci. Lett. 168, 219–232.

Feng, Z.D., Ran, M., Yang, Q.L., Zhai, X.W., Wang, W., Zhang, X.S., Huang, C.Q., 2011. Stratigraphies and chronologies of late Quaternary loess–paleosol sequences in the core area of the central Asian arid zone. Quat. Int. 240, 156–166.

Fitzsimmons, K.E., Sprafke, T., Zielhofer, C., Günter, C., Deom, J.-M., Sala, R., Iovita, R., 2017. Loess accumulation in the Tian Shan piedmont: implications for palaeoenvironmental change in arid Central Asia. Quat. Int. in press, http://dx.doi.org/10.1016/j.quaint.2016.07.041.

Gorbarenko, S.A., Goldberg, E.L.V., Kashgarian, M., Velivetskaya, T.Y.A., Zakharkov, S.P., Pechnikov, V.S., Bosin, A.A.E., Psheneva, O.Y.E., Ivanova, E.D., 2007. Millennium scale environment changes of the Okhotsk Sea during last 80 kyr and their phase relationship with global climate changes. J. Oceanogr. 63, 609–623.

Heinrich, H., 1988. Origin and consequences of cyclic ice rafting in the Northeast Atlantic Ocean during the past 130,000 years. Quat. Res. 29, 142–152.

Hu, L.J., 2004. Physical Geography of the Tianshan Mountains in China. China Environmental Science Press, Beijing (in Chinese).

Jeong, G.Y., Hillier, S., Kemp, R.A., 2008. Quantitative bulk and single-particle mineralogy of a thick Chinese loess–paleosol section: implications for loess provenance and weathering. Quat. Sci. Rev. 27, 1271–1287.

Jeong, G.Y., Hillier, S., Kemp, R.A., 2011. Changes in mineralogy of loess–paleosol sections across the Chinese Loess Plateau. Quat. Res. 75, 245–255.

Kang, S., Wang, X., Lu, Y., Liu, W., Song, Y., Wang, N., 2015. A high-resolution quartz OSL chronology of the Talede loess over the past ~30 ka and its implications for dust accumulation in the Ili Basin, Central Asia. Quat. Geochronol. 30, 181–187.

Li, J.F., 1991. Climate in Xinjiang. China Meteorological Press, Beijing (in Chinese).

Li, C.X., Song, Y.G., 2011. Application of grain-size age models on Zhaosu loess stratigraphy in the Ili region. J. Earth Environ. 2, 612–617 (in Chinese with English abstract).

Li, C.X., Song, Y.G., Qian, L.B., Wang, L.M., 2011. The history of climate change recorded by the grain size at the Zhaosu loess section in the Central Asia since the last glacial period. Acta Sed. Sini. 29, 866–873 (in Chinese with English abstract).

Li, Y., Song, Y., Yan, L., Chen, T., An, Z., 2015. Timing and spatial distribution of loess in Xinjiang, NW, China. PLoS ONE 10, e0125492.

Li, Y., Song, Y., Lai, Z., Han, L., An, Z., 2016a. Rapid and cyclic dust accumulation during MIS 2 in Central Asia inferred from loess OSL dating and grain-size analysis. Sci. Rep. 6, e32365. doi: 32310.31038/srep32365.

Li, Y., Song, Y.G., Zhao, J.D., 2016b. Micromorphological characters of quartz grain from Nilke loess-paleosol sequences and their implications of origin and provenance. J. Earth Environ. 7, 366–379 (in Chinese with English abstract).

Li, Y., Song, Y., Zeng, M., Lin, W., Orozbaev, R., Cheng, L., Chen, X., Halmurat, T., 2017. Evaluating the paleoclimatic significance of clay mineral records from a late Pleistocene loess-paleosol section of the Ili Basin, Central Asia. Quat. Res., in press, http://dx.doi.org/10.1017/qua.2017.58.

Liu, T.S., 1985. Loess and the Environment. China Ocean Press, Beijing, pp. 1–251.

Liu, Y., Shi, Z., Deng, C., Su, H., Zhang, W., 2012. Mineral magnetic investigation of the Talede loess-palaeosol sequence since the last interglacial in the Yili Basin in the Asian interior. Geophys. J. Int. 190, 267–277.

Lu, H., An, Z., 1998a. Pretreated methods on loess-palaeosol samples granulometry. Chin. Sci. Bull. 43, 237–240.

Lu, H.Y., An, Z.S., 1998b. Paleoclimatic significance of grain size of loess-palaeosol deposit in Chinese Loess Plateau. Sci. China Ser. D – Earth Sci. 41, 626–631.

Lu, L.Q., Fang, X.M., Lu, H.Y., Han, Y.X., Yang, S.L., Li, J.J., An, Z.S., 2004. Millennial-scale climate change since the last glaciation recorded by grain sizes of loess deposits on the northeastern Tibetan Plateau. Chin. Sci. Bull. 49, 1157–1164.

Machalett, B., Oches, E.A., Frechen, M., Zöller, L., Hambach, U., Mavlyanova, N.G., Marković, S.B., Endlicher, W., 2008. Aeolian dust dynamics in central Asia during the Pleistocene: driven by the long-term migration, seasonality, and permanency of the Asiatic polar front. Geochem. Geophys. Geosys. 9, 1–22.

NGRIP_members, 2004. High-resolution record of Northern Hemisphere climate extending into the last interglacial period. Nature 431, 147–151.

Nie, J., Stevens, T., Rittner, M., Stockli, D., Garzanti, E., Limonta, M., Bird, A., Andò, S., Vermeesch, P., Saylor, J., Lu, H., Breecker, D., Hu, X., Liu, S., Resentini, A., Vezzoli, G., Peng, W., Carter, A., Ji, S., Pan, B., 2015. Loess Plateau storage of Northeastern Tibetan Plateau-derived Yellow River sediment. Nat. Commun. 6, 8511 doi: 8510.1038/ncomms9511.

Porter, S.C., An, Z.S., 1995. Correlation between climate events in the North Atlantic and China during the last glaciation. Nature 375, 305–308.

Rao, Z., Chen, F., Cheng, H., Liu, W., Wang, G.A., Lai, Z., Bloemendal, J., 2013. High-resolution summer precipitation variations in the western Chinese Loess Plateau during the last glacial. Sci. Rep. 3, e2785.

Rasmussen, S.O., Bigler, M., Blockley, S.P., Blunier, T., Buchardt, S.L., Clausen, H.B., Cvijanovic, I., Dahl-Jensen, D., Johnsen, S.J., Fischer, H., Gkinis, V., Guillevic, M., Hoek, W.Z., Lowe, J.J., Pedro, J.B., Popp, T., Seierstad, I.K., Steffensen, J.P., Svensson, A.M., Vallelonga, P., Vinther, B.M., Walker, M.J.C., Wheatley, J.J., Winstrup, M., 2014. A stratigraphic framework for abrupt climatic changes during the Last Glacial period based on three synchronized Greenland ice-core records: refining and extending the INTIMATE event stratigraphy. Quat. Sci. Rev. 106, 14–28.

Rousseau, D.-D., Antoine, P., Kunesch, S., Hatté, C., Rossignol, J., Packman, S., Lang, A., Gauthier, C., 2007. Evidence of cyclic dust deposition in the US Great plains during the last deglaciation from the high-resolution analysis of the Peoria Loess in the Eustis sequence (Nebraska, USA). Earth Planet. Sci. Lett. 262, 159–174.

Schulz, H., von Rad, U., Erlenkeuser, H., 1998. Correlation between Arabian Sea and Greenland climate oscillations of the past 110,000 years. Nature 393, 54–57.

Seierstad, I.K., Abbott, P.M., Bigler, M., Blunier, T., Bourne, A.J., Brook, E., Buchardt, S.L., Buizert, C., Clausen, H.B., Cook, E., Dahl-Jensen, D., Davies, S.M., Guillevic, M., Johnsen, S.J., Pedersen, D.S., Popp, T.J., Rasmussen, S.O., Severinghaus, J.P., Svensson, A., Vinther, B.M., 2014. Consistently dated records from the Greenland GRIP, GISP2 and NGRIP ice cores for the past 104 ka reveal regional millennial-scale δ18O gradients with possible Heinrich event imprint. Quat. Sci. Rev. 106, 29–46.

Shi, Z.T., Dong, M., 2007. Characteristics of loess grain size and source of dust in Tian Shan, China. J. Yunnan Normal Univ. (Nat. Sci.) 27, 55–57 (in Chinese with English abstract).

Shi, Z.T., Dong, M., Fang, X.M., 2007. The characteristics of Late Pleistocene loess-paleosol magnetic susceptibility in Yili Basin. J. Yunnan Normal Univ. (Nat. Sci.) 43, 7–10 (in Chinese with English abstract).

Smalley, I.J., Mavlyanova, N.G., Rakhmatullaev, K.L., Shermatov, M.S., Machalett, B., O'Hara Dhand, K., Jefferson, I.F., 2006. The formation of loess deposits in the Tashkent region and parts of Central Asia; and problems with irrigation, hydro-collapse and soil erosion. Quat. Int. 152–153, 59–69.

Song, Y.G., 2012. Paleoclimatic implication of temperature-dependence of susceptibility of Tianshan loess, Central Asia. Adv. Sci. Lett. 6, 167–172.

Song, Y.G., Shi, Z.T., Fang, X.M., Nie, J.S., Naoto, I., Qiang, X.K., Wang, X.L., 2010. Loess magnetic properties in the Ili Basin and their correlation with the Chinese Loess Plateau. Sci. China Earth Sci. 53, 419–431.

Song, Y.G., Li, C.X., Zhao, J.D., Cheng, P., Zeng, M.X., 2012. A combined luminescence and radiocarbon dating study of the Ili loess, Central Asia. Quat. Geochronol. 10, 2–7.

Song, Y.G., Chen, X.L., Qian, L.B., Li, C.X., Li, Y., Li, X.X., Chang, H., An, Z.S., 2014. Distribution and composition of loess sediments in the Ili Basin, Central Asia. Quat. Int. 334, 61–73.

Song, Y., Lai, Z., Li, Y., Chen, T., Wang, Y., 2015. Comparison between luminescence and radiocarbon dating of late Quaternary loess from the Ili Basin in Central Asia. Quat. Geochronol. 30, 405–410.

Song, Y.G., Li, Y., Li, Y., An, Z., Cheng, L., Sun, H., Rustam, O., 2017. North Atlantic Abrupt climate signals during the last glacial period in Central Asia: evidences from aeolian loess sediments. Acta Geol. Sin-Engl. 91, 1135–1136.

Sun, J., 2002. Source regions and formation of the loess sediments on the high mountain regions of Northwestern China. Quat. Res. 58, 341–351.

Sun, D.H., Bloemendal, J., Rea, D.K., An, Z.S., Vandenberghe, J., Lu, H.Y., Su, R.X., Liu, T.S., 2004. Bimodal grain-size distribution of Chinese loess, and its palaeoclimatic implications. CATENA 55, 325–340.

Sun, Y., Lu, H.Y., An, Z.S., 2006. Grain size of loess, palaeosol and Red Clay deposits on the Chinese Loess Plateau: significance for understanding pedogenic alteration and palaeomonsoon evolution. Palaeogeog. Palaeoclimatol. Palaeoecol. 241, 129–138.

Sun, Y.B., Clemens, S.C., Morrill, C., Lin, X.P., Wang, X.L., An, Z.S., 2012. Influence of Atlantic meridional overturning circulation on the East Asian winter monsoon. Nat. Geosci. 5, 46–49.

Thompson, L.G., Yao, T., Davis, M.E., Henderson, K.A., Thompson, E.M., Lin, P.N., Beer, J., Synal, H.A., Cole-Dai, J., Bolzan, J.F., 1997. Tropical climate instability: the last glacial cycle from a qinghai-tibetan ice core. Science 276, 1821–1825.

Wen, Q.Z., 1989. Loess Geochemistry in China. Chinese Science press, Beijing (In Chinese).

Xiao, J., Porter, S.C., An, Z., Kumai, H., Yoshikawa, S., 1995. Grain size of quartz as an indicator of winter monsoon strength on the loess plateau of central China during the Last 130,000 Yr. Quat. Res. 43, 22–29.

Yang, J., Chen, J., An, Z., Shields, G., Tao, X., Zhu, H., Ji, J., Chen, Y., 2000. Variations in 87Sr/86Sr ratios of calcites in Chinese loess: a proxy for chemical weathering associated with the East Asian summer monsoon. Palaeogeog. Palaeoclimatol. Palaeoecol. 157, 151–159.

Yang, S.L., Forman, S.L., Song, Y.G., Pierson, J., Mazzocco, J., Li, X.X., Shi, Z.T., Fang, X.M., 2014. Evaluating OSL-SAR protocols for dating quartz grains from the loess in Ili Basin, Central Asia. Quat. Geochronol. 20, 78–88.

Ye, W., 2001. Sedimentary Characteristics of Loess and Paleoclimate in Westerly Region of Xinjiang. China Ocean press, Beijing (in Chinese).

Ye, W., Dong, G.R., Yuan, Y.J., Ma, Y.J., 2000. Climate instability in the Yili region, Xinjiang during the last glaciation. Chin. Sci. Bull. 45, 1604–1609.

Zeeden, C., Hambach, U., Veres, D., Fitzsimmons, K., Obreht, I., Bösken, J., Lehmkuhl, F., 2017. Millennial scale climate oscillations recorded in the Lower Danube loess over the last glacial period. Palaeogeog. Palaeoclimatol. Palaeoecol., in press, http://dx. doi.org/10.1016/j.palaeo.2016.12.029.

Zeng, M.X., Song, Y.G., 2012. Study on the influencing factors of the Levenberg-Marquardt Algorithm for X-ray diffraction quantitative phase analysis. Rock Mineral Anal. 31, 798–806 (in Chinese with English abstract).

Zeng, M.X., Song, Y.G., 2013a. Application of the Levenberg-Marquardt Algorithm to X-ray diffraction quantitative phase analysis. Earth Sci.-J. China Univ. Geosci. 38, 331–340 (in Chinese with English abstract).

Zeng, M.X., Song, Y.G., 2013b. Carbonate minerals of Zhaosu loess section in westerly area and their paleoenvironmental significance. Quat. Sci. 33, 424–436 (in Chinese with English abstract).

Zhang, W.X., Shi, Z.T., Chen, G.J., Liu, Y., Niu, J., Ming, Q.Z., Su, H., 2013. Geochemical characteristics and environmental significance of Talede loess–paleosol sequences of Ili Basin in Central Asia. Environ. Earth Sci. 70, 2191–2202.

Zhao, K., Li, X., Dodson, J., Zhou, X., Atahan, P., 2013. Climate instability during the last deglaciation in central Asia, reconstructed by pollen data from Yili Valley, NW China. Rev. Palaeobot. Palyno. 189, 8–17.